Microchimica Acta
https://doi.org/10.1007/s00604-018-3193-8

ORIGINAL PAPER

Colorimetric and visual mercury(II) assay based on target-induced cyclic enzymatic amplification, thymine-Hg(II)-thymine interaction, and aggregation of gold nanoparticles

Xiaolei Song[1] · Yu Wang[2] · Su Liu[1] · Xue Zhang[2] · Haiwang Wang[2] · Jingfeng Wang[2] · Jiadong Huang[2,3]

Received: 10 December 2018 / Accepted: 20 December 2018

Abstract
A colorimetric biosensor and visual test is described for the determination of mercury(II). It relies on the specific thymine-Hg(II)-thymine (T-Hg^{2+}-T) interaction which induces a cyclic amplification process (caused by the enzyme exonuclease III) and the aggregation of gold nanoparticles. These results in a color change from red to violet. Under optimized conditions, this colorimetric assay (best performed at 524 nm) has a detection limit as low as 0.9 nM with a detection range over 4 orders of magnitude (from 1 nM to 10 μM).

Keywords Mercury ion · T-Hg^{2+}-T · Exonuclease III · AuNPs · Visual detection · UV-vis absorption

Introduction

Mercury is one of the ten most hazardous heavy metals, and its bioaccumulation can cause severe health problems in living organisms at very low concentrations [1–3]. The solvated mercury ion (Hg^{2+}) is the major stable form in natural world because its significant water solubility [4]. The maximum allowable concentration of Hg^{2+} in drinking water mandated by the United States Environmental Protection Agency (EPA) is about 2 ppb (10 nM) [5]. Conventional techniques for Hg^{2+} quantification, for example, atomic absorption spectrometry (AAS) [6] and atomic fluorescence spectrometry (AFS) [7] are widely used. Although they offer high accuracy, these methods require time-consuming sample pretreatment and skilled personnel, which limit their applications for on-site detection [8, 9]. Hence, it is urgent to address these challenges, and especially to develop convenient methods for aqueous Hg^{2+} detection.

Colorimetric detection of Hg^{2+} has drawn considerable interest [10–12]. In particular, newly reported colorimetric biosensors, which combine the unique optical properties of gold nanoparticles (AuNP) with the coordinate interaction of thymine-Hg^{2+}-thymine (T-Hg^{2+}-T), present revolutionary strategies for Hg^{2+} assay [13, 14]. For instance, Lee and co-workers developed a chip-based scanometric method for Hg^{2+} using DNA-functionalized AuNP, with a limit of detection of 10 nM for 2 h [15]. Chen reported a disposable strip biosensor for visual detection of Hg^{2+} based on target-triggered toehold binding and exonuclease III (Exo III)-assisted signal amplification, with three steps for 65 min [16]. Liu and co-workers studied an enzyme-free colorimetric biosensor for Hg^{2+}, taking advantage of strand displacement amplification and DNA conjugated to AuNP, which achieved nanomolar sensitivity (3.4 nM) for 1 h [17]. Hong also reported a colorimetric method for detection of Hg^{2+} using Exo III-assisted target recycling and AuNP, with three steps for 100 min [18]. Although their widespread availability, the shortcomings of time-consuming, multistep protocols, or lacking of enough accuracy for on-site screening and point-of-care (POC) diagnostics in environmental samples need to be further overcame.

Herein, we describe a one-step, homogeneous, and colorimetric method for highly sensitive and selective detection of

Electronic supplementary material The online version of this article (https://doi.org/10.1007/s00604-018-3193-8) contains supplementary material, which is available to authorized users.

✉ Jiadong Huang
chm_huangjd@ujn.edu.cn

[1] School of Water Conservancy and Environment, University of Jinan, Jinan 250022, People's Republic of China

[2] College of Biological Sciences and Technology, University of Jinan, Jinan 250022, People's Republic of China

[3] Key Laboratory of Chemical Sensing & Analysis in Universities of Shandong, College of Chemistry and Chemical Engineering, University of Jinan, Jinan 250022, People's Republic of China

Published online: 12 January 2019

Hg^{2+} based on target-induced cyclic enzymatic amplification, T-Hg^{2+}-T interaction and aggregation of AuNP. AuNP is widely used as a signal indicator due to its high extinction coefficient in the visible region and distance-dependent optical properties [19–21]. This colorimetric assay depends on the Exo III-mediated aggregation of AuNP that is attributed to the specific T-Hg^{2+}-T interaction, thus the color and absorbance output with quantitatively correlated to target Hg^{2+} can be directly observed by the bare eye and UV-Vis spectroscopy. On the basis of Exo III-assisted target recycling and cyclic cleavage of AuNP, the colorimetric method can offer the advantages of simplified operation (one step), shortened detection time (30 min), and improved sensitivity (0.9 nM). As a result, the studied colorimetric biosensor indeed creates an useful and commodious platform for visualized detection of Hg^{2+} in aqueous systems.

Materials and methods

Reagents and materials

Oligonucleotides used in this work were purchased from Sangon Biotechnology Co. Ltd. (Shanghai, China; https://www.sangon.com/) and were purified via HPLC. The sequences of these oligonucleotides are listed in Tab. S1. $Hg(NO_3)_2$, trisodium citrate and chloroauric acid ($HAuCl_4 \cdot 4H_2O$) were purchased from Aladdin Chemistry Co., Ltd. (Shanghai, China; http://www.aladdin-e.com/). Exonuclease III (Exo III) and NEBuffer 1 were purchased from New England Biolabs Inc. (Beijing, China; http://www.neb-china.com/). Phosphate buffer (PB, 100 mM, pH 7.4), and phosphate-buffered saline (PBS, 10 mM, pH 7.4) were from Sigma-Aldrich (St. Louis, MO; https://www.sigmaaldrich.com/). All other reagents were of analytical reagent grade and purchased from Sinopharm Chemical Reagent Co. Ltd. (Beijing, China; https://www.sinoreagent.com/) and were used without further purification. All solutions were prepared with ultrapure water that was conducted using a Millipore Milli-Q water purification system (Billerica, MA, USA; http://www.merckmillipore.com/) with an electric resistance >18 MΩ cm (https://en.wikipedia.org/wiki/Electrical_resistivity_and_conductivity).

Apparatus

Absorption spectra were conducted on a UV2600 UV-vis spectrophotometer (Shimadzu international trading Co. Ltd., Japan; http://www.shimadzu.com.cn/) at room temperature. Transmission electron microscopy (TEM) measurements were carried out using a JEM-3010 transmission electron microscope (http://www.jeol.co.jp/). The samples for TEM characterization were prepared by adding a drop of colloidal solution on a carbon-coated copper grid and then drying at room temperature.

Analytical protocol

The detailed procedure was as follows: Before the experiment, the same volumes of C (100 μM) and L* (100 μM) were sufficiently mixed. Then, the mixture was incubated at 95 °C for 5 min and cooled down to room temperature for at least 30 min, and the cooled mixture was the C-L* hybrid duplex. Subsequently, C-L* hybrid duplex (4 μL, 5 μM), C* (2 μL, 0.5 μM), NEBuffer 1 (4 μL, 1×), ultrapure water (26 μL), Exo III (2 μL, 5 U), the prepared L-AuNP (20 μL, 1 nM; the preparation of AuNP and L-AuNP were given in the

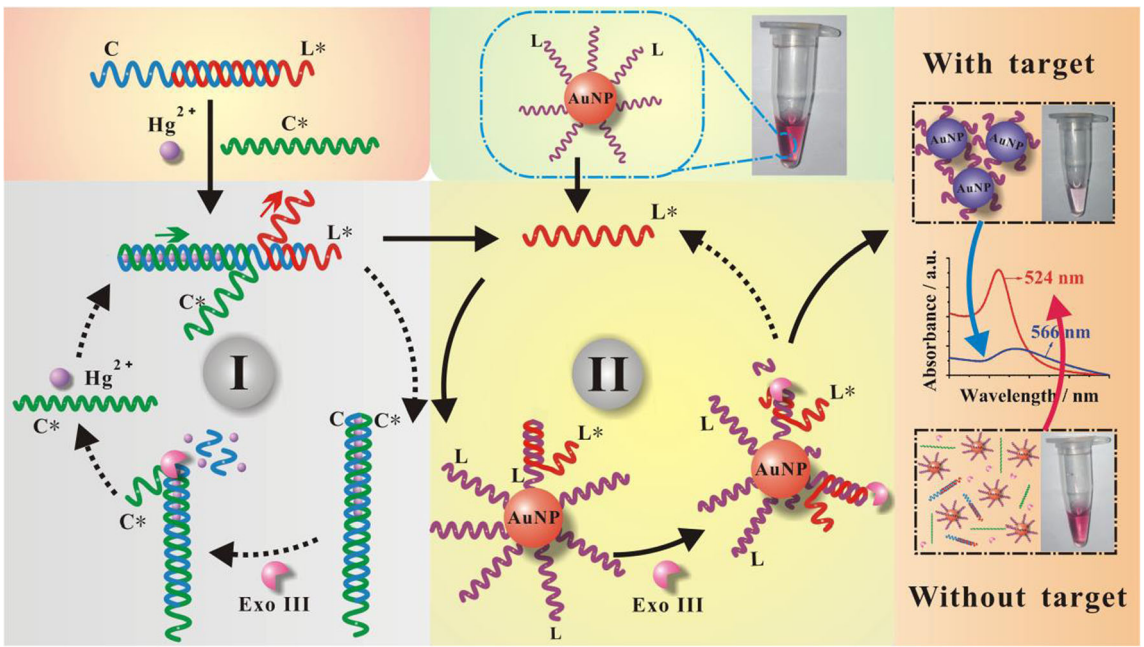

Scheme 1 Schematic illustration of the colorimetric assay of Hg^{2+}

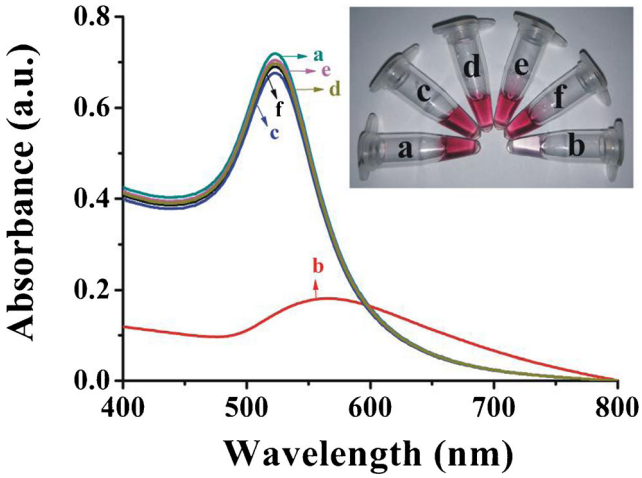

Fig. 1 Absorption spectra responses for colorimetric assay of Hg^{2+}. Curves a, c to e are for the control experiments which were performed in the absence of Hg^{2+} (blank sample) **a**, C* **c**, L* **d**, or Exo III **e**, in the presence of non-target Pb^{2+} in place of Hg^{2+} **f**. Colorimetric responses of the biosensor performed upon analyzing 10 μM Hg^{2+} (positive sample) **b**. The inset shows the corresponding color changes

Electronic Supplementary Material) and 2 μL of Hg^{2+} (or other heavy metal ions or unknown samples) with different concentrations (ranging from 1 nM to 10 μM) were mixed and incubated for 30 min at 37 °C. Subsequently, the color change was observed and the absorbance spectrum of reaction product (60 μL) was detected by UV-visible spectrometer in the wavelength range from 400 nm to 800 nm. And the absorbance at 524 nm was used for quantitative analysis.

Results and discussion

Principle of the assay

Scheme 1 shows the working principle of the reported biosensor. A short single-strand DNA (L)-modified AuNP (L-AuNP) is pre-prepared according to the previously reported methods [22], in which the modification of L on AuNP surface is fulfilled via Au-S covalent bond. A hybrid duplex DNA (C-L*) is ingenious designed by hybridizing a capture probe (C) that is rich in thymine at 3′-terminus with L-annealing DNA probe (L*). The two 3′ termini of the DNA duplex are protruding in order to be protected from Exo III-catalyzed degradation. Our colorimetric reaction system consists of the DNA duplex C-L*, L-AuNP, Exo III, and the thymine-rich DNA (C*) that is complementary with part of C. After the addition of target Hg^{2+} into the system, C-L* and C* can serve as the specific recognition elements for Hg^{2+} via T-Hg^{2+}-T coordination chemistry, resulting in the hybridization of C with C*, that L* is squeezed down and the C-C* duplex with a 3′ blunt end is produced. Then C of the C-C* duplex is cleaved into fragments from the 3′-terminus owing to the excellent activity of Exo III on DNA duplexes [23, 24], resulting in the release of Hg^{2+} and C*. Subsequently, a new cycle of "recognition-hybridization-cleavage" occurs with the aid of Exo III, which constitutes the Cycle I. So, a great abundant of dissociative L* are generated after Exo III-mediated target recycling amplification reaction, which can combine with the L-AuNPs and form the L-L* duplex with a blunt 3′-terminus. Thus the cyclic degradation of L on AuNP by Exo III is activated (This constitutes the Cycle II), initiating the aggregation of AuNP that accompany with a color change from red to violet, which is attributed to the distance change between AuNP. However, in the absence of Hg^{2+}, the Exo III-aided cleavage process cannot be activated, thus there are no changes for the color and UV-Vis absorption intensity of AuNP. The changes of color and absorbance of the AuNP correspond to the Hg^{2+}-initiated enzymic amplification reaction. Therefore, they can be used for detection of Hg^{2+} concentration.

Viability of the strategy

To confirm the feasibility of this strategy, a series of control experiment were performed, and the results are shown in Fig. 1. For the blank sample, it is found that a strong absorption peak appears at 524 nm and the absorption intensity is 0.719,

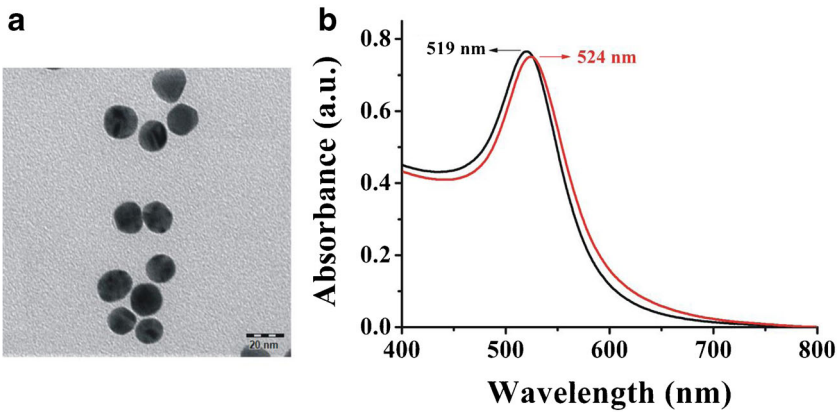

Fig. 2 **a** TEM micrograph of the prepared AuNP; **b** Normalized UV-Vis spectra of the bare AuNP (black curve) and the L-AuNPs (red curve)

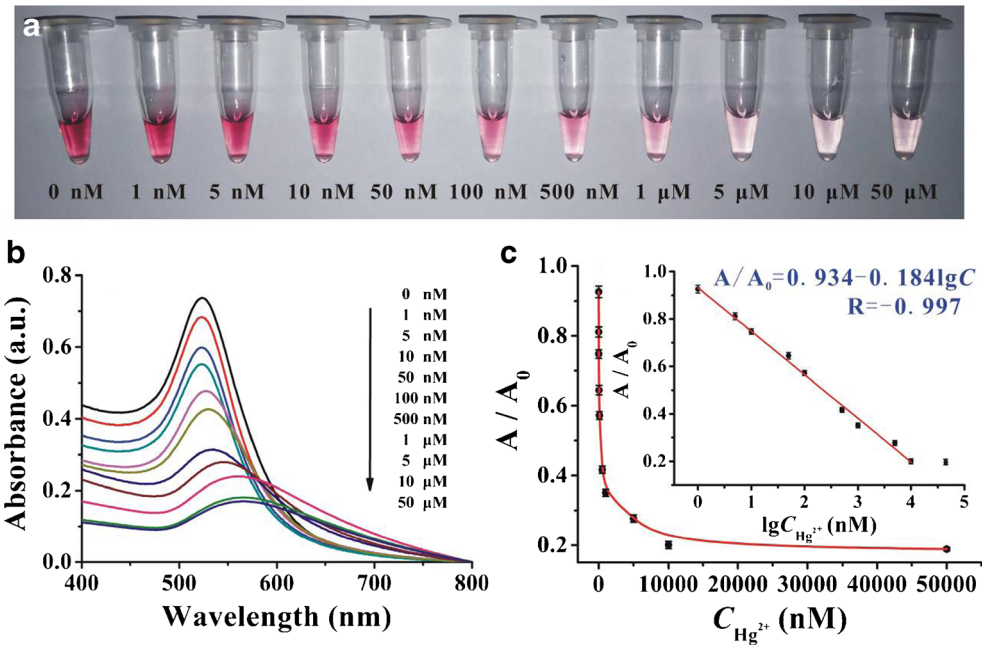

Fig. 3 **a** Photograph and **b** absorption spectra responses of the strategy in response to different concentrations of Hg^{2+}; **c** The plot of (A/A_0) vs. the Hg^{2+} concentration for direct assay. Inset: the relationship between A/A_0 and the logarithm of concentration of Hg^{2+} (1 nM to 10 μM). Error bars show the standard deviations of three repetitive experiments

suggesting the AuNP can well disperse in the buffer (curve a). In contrast, the absorption intensity of AuNP at 524 nm is significantly decreased, and a new absorption peak at ~566 nm is observed that corresponds to the AuNP aggregates for the positive sample (curve b). This indicates the specific binding of target Hg^{2+} initiate Exo III-assisted enzymatic amplification reaction and aggregation of AuNP, thus there are an obvious color change of AuNP and a significant change of absorption peak. More control experiments were performed to further validate the design. In the absence of C*, the absorption peak is located at 524 nm. It is attributed to the coexistence of C-L* and Hg^{2+}. Thus, L* cannot anneal with L-AuNP (curve c). This implies only the simultaneous binding of Hg^{2+} to C-L* and C* via T-Hg^{2+}-T coordination chemistry can induce the release of L*. Additionally, for the samples that losing L* (curve d) and Exo III (curve e), respectively, their absorption spectra are similar to that of the blank sample, signifying the colorimetric assay is dependent on the combined action of C-L*, C*, Exo III, and L-AuNP. Furthermore, when the target was replaced by non-target Pb^{2+}, we observe a powerful absorption signal (curve f), demonstrating the changes of AuNP color and absorption peak are induced by target Hg^{2+}. On the basis of these results, it is reasonably concluded that the reported strategy may be used for the amplified colorimetric detection of Hg^{2+}.

Characterization of the bare AuNPs and the ssDNA modified AuNPs (L-AuNPs)

Transmission electron microscopy (TEM) and UV-Vis spectroscopy were utilized to investigate the prepared AuNP and

Table 1 Detection performance comparison of our assay with other methods

Materials [a]	Methods [b]	Linear range (nM)	LOD (nM)	Time / Steps	Disadvantages	Ref.
GO	F	3.0×10^0–3.5×10^2	1.00×10^{-1}	8 min / 3 steps	Multistep protocols	[25]
WS_2	F	6.0×10^0–6.5×10^2	3.30×10^0	35 min / 3 steps	Multistep protocols	[26]
CDs	F	4.0×10^3–1.8×10^4	2.47×10^3	- / 1 step	Poor sensitivity	[27]
Rho-MCS	F	5.0×10^2–7.0×10^3	1.50×10^1	- / 1 step	Relatively poor sensitivity	[28]
AgNP/GO	C	1.0×10^4–2.0×10^5	3.38×10^2	- / 1 step	Poor sensitivity	[29]
AgNP/GO	C	–	5.90×10^2	2 min / 1 step	Poor sensitivity	[30]
AuNP/S-CDs	C	5.0×10^1–1.0×10^3	4.70×10^1	60 min / 2 steps	Relatively time-consuming and poor sensitivity	[31]
DNA-AuNP	C	5.0×10^0–1.0×10^4	3.40×10^0	60 min / 2 steps	Relatively time-consuming	[17]
DNA-AuNP	C	1.0×10^0–1.0×10^4	9.00×10^{-1}	30 min / 1 step	Relatively costly	This work

[a] *GO* graphene oxide, *WS_2* layered tungsten disulfide nanosheets, *CDs* carbon dots, *Rho-MCS* rhodamine magnetic chitosan microspheres, *AgNP* silver nanoparticles, *S-CDs* sulfur-doped carbon nanodots

[b] *F* fluorometry, *C* colorimetry

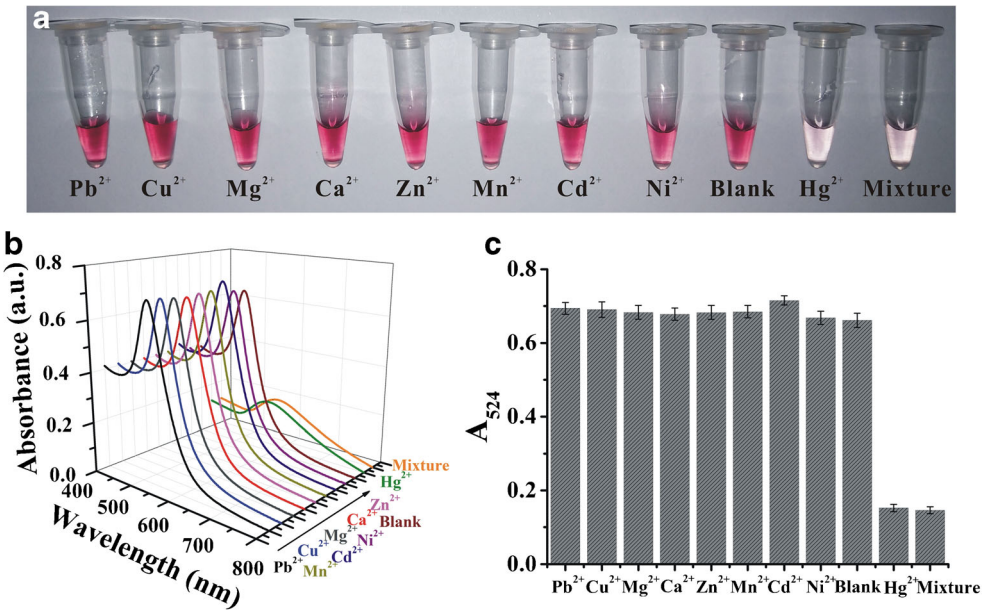

Fig. 4 **a** Photographs of the ssDNA modified AuNPs (L-AuNPs) in response to different metal ions; **b** Absorption spectra and **c** absorbance value of A_{524} of the biosensor toward different metal ions. Concentrations of Hg^{2+} and other metal ions are 10 μM and 5 mM, respectively. The mixture contains 10 μM Hg^{2+} and 5 mM other metal ions. Error bars are standard deviations across three repetitive experiments

L-AuNPs. It is observed from Fig. 2a that the prepared AuNP exhibits good monodispersity, almost round shape, and homogeneous size. As demonstrated by UV-Vis spectroscopy in Fig. 2b, the bare AuNP (~20 nm diameter) shows maximum absorbance at 519 nm (black curve), while the absorption peak of L-AuNPs displays an obvious red shift (~5 nm), indicating the successful modification of L probe on AuNP surface (red curve).

Analytical performance

To achieve an optimal analytical performance of the biosensor for Hg^{2+} detection, some key experimental parameters, e.g. the concentrations of Exo III (5 units), C-L* hybrid duplex (5 μM), C* (0.5 μM), and L-AuNPs (1 nM), and the reaction time for enzymatic cleavage (30 min), were investigated in detail in Fig. S1 in the Electronic Supplementary Material. Under the optimal experimental conditions, the constructed colorimetric method was adopted for the determination of Hg^{2+} at various concentrations (Fig. 3). It is observed in Fig. 3a that the red color of the L-AuNPs is gradually attenuated with increasing concentration of Hg^{2+}, suggesting that the L-AuNPs are assembled into larger aggregates in the presence of higher Hg^{2+} concentrations. The absorbance intensity at 524 nm gradually decreases and also more and more red shift with the increasing concentrations of Hg^{2+} (Fig. 3b), which is consistent with that of the visual observations. As shown in Fig. 3c, the A/A_0 value continues to decrease with the increase of Hg^{2+} concentration from 0 nM to 50 μM until reach a plateau when the concentration is 10 μM, where A and A_0 are the absorbance signal at 524 nm in the presence and absence of Hg^{2+}, respectively. Additionally, plot of A/A_0 exhibits a good linear correlation to the logarithm of the concentrations of Hg^{2+} ranging from 1 nM to 10 μM (inset in Fig. 3c). The linear regression equation is $A/A_0 = 0.934–0.184\ \lg C$, with a correlation coefficient (R) of −0.997, and C represents the concentration of Hg^{2+} (nM). The limit of detection (LOD) of 0.90 nM is calculated by evaluating the average response of blank sample plus 3 times standard deviation. The analytical performance of our strategy for quantitative assay of Hg^{2+} was compared with that of some earlier reported methods. The results are shown in Table 1. It is found that our biosensor offers the relatively high sensitivity, shortened analysis time and simplified operation with only one-step homogeneous reaction as compared to the previously methods for detecting Hg^{2+}. Therefore, these results indicate the studied colorimetric method may be used for Hg^{2+} quantification.

Table 2 Detection of Hg^{2+} in tap water samples by our strategy and AFS

Sample	Hg^{2+} Added (μM)	Hg^{2+} Detected (μM)		Recovery (%)	
		Biosensor (±SD, $n = 4$)	AFS (±SD, n = 4)	Biosensor	AFS
Tap water 1	1.000×10^{-2}	$(1.031 \pm 0.024) \times 10^{-2}$	$(0.976 \pm 0.037) \times 10^{-2}$	103.1	97.6
Tap water 2	1.000×10^{-1}	$(0.912 \pm 0.035) \times 10^{-1}$	$(1.038 \pm 0.025) \times 10^{-1}$	91.2	103.8
Tap water 3	1.000×10^{0}	$(1.059 \pm 0.021) \times 10^{0}$	$(1.027 \pm 0.022) \times 10^{0}$	105.9	102.7

Selectivity

In order to evaluate the specificity of this protocol, we investigated the selectivity of this biosensor by detecting Hg^{2+} (10 μM) and other non-target heavy metal ions (5 mM), including Pb^{2+}, Cu^{2+}, Mg^{2+}, Ca^{2+}, Zn^{2+}, Mn^{2+}, Cd^{2+} and Ni^{2+}, under optimum conditions. The results are shown in Fig. 4. It can be seen that the presence of the non-target metal ions cannot cause any obvious color change (Fig. 4a) and absorbance signal change (Fig. 4b, c) compared with that of the blank sample, while the addition of Hg^{2+} results in a attenuated red color (Fig. 4a) of the AuNP solution, and shows a remarkable change of absorbance (Fig. 4b, c). Such excellent specificity of this assay can be attributed to the specific T-Hg^{2+}-T base pairing. When Hg^{2+} was coexisted with the non-target metal ions, no significant change is observed compared to the Hg^{2+} existed alone. The result confirms that other heavy metal ions cannot interfere with the detection of Hg^{2+}. Accordingly, the colorimetric method has a high selectivity for Hg^{2+} in environmental samples that various metal ions are coexisted.

Environmental sample analysis

To evaluate the practical applicability, our biosensor was carried out in the detection of Hg^{2+} with tap water. The concentration of Hg^{2+} in tap water was too low to be detected, so the samples were respectively spiked with 10 nM, 100 nM, 1000 nM of Hg^{2+} standard solution according to the general procedure. To test the accuracy of our methods, atomic fluorescence spectroscopy (AFS) was also used for the detection of the same samples. The results are summarized in Table 2. As can be seen, these values measured by this method are in good agreement with the data determined by AFS, and the discrepancies between these two methods are all smaller than 12.6%. These results clearly demonstrate that our established colorimetric method may be applied for the practical environmental samples analysis with excellent reliability and accuracy.

Conclusion

We report a colorimetric biosensor for Hg^{2+} based on target-induced cyclic enzymatic amplification, thymine-Hg(II)-thymine interaction and aggregation of gold nanoparticles. On the basis of the multiple recycling amplification strategy, this colorimetric strategy obtains improved sensitivity with a detection limit of 0.90 nM in drinking water. Furthermore, this constructed strategy sustains a remarkable selectivity for Hg^{2+} against other possible background ions. In addition, this assay offers the advantage of shortened analysis time, simplified operation with only one-step homogeneous reaction. Moreover, the decrease of cost for detection will be also included in the future work to develop a versatile and low-cost biosensing platform.

Acknowledgements This work was supported by National Natural Science Foundation of China (31471644), the Primary Research & Development Plan of Shandong Province (2017GSF220009). University of Jinan Scientific Research Fund (Youth Project XKY1421) and Doctoral Fundation of University of Jinan (XBS1431).

Compliance with ethical standards The author(s) declare that they have no competing interests.

References

1. Huang DW, Niu CG, Wang XY, Lv XX, Zeng GM (2013) "Turn-on" fluorescent sensor for Hg^{2+} based on single-stranded DNA functionalized Mn:CdS/ZnS quantum dots and gold nanoparticles by time-gated mode. Anal Chem 85(2):1164–1170
2. Bi N, Hu MH, Xu J, Jia L (2017) Colorimetric determination of mercury (II) based on the inhibition of the aggregation of gold nanorods coated with 6-mercaptopurine. Microchim Acta 184(10):3961–3967
3. Liu YC, Wang XQ, Wu H (2017) Reusable DNA-functionalized-graphene for ultrasensitive mercury (II) detection and removal. Biosens Bioelectron 87:129–135
4. Chen YJ, Yao L, Deng Y, Pan DD, Ogabiela E, Cao JX, Adeloju SB, Chen W (2015) Rapid and ultrasensitive colorimetric detection of mercury (II) by chemically initiated aggregation of gold nanoparticles. Microchim Acta 182(13–14):2147–2154
5. Office of Water (2001) Mercury update: impact on fish advisories, EPA fact sheet EPA-823-F-01-011. U.S. In: Environmental Protection Agency. D. C, Washington
6. Zenko Y, Masao T (1977) Indirect determination of submicrogram amounts of sulfide by flameless atomic absorption spectrometry of mercury. Microchim Acta 67(5–6):459–468
7. Guzmán-Mar JL, Hinojosa-Reyes L, Serra AM, Hernández-Ramírez A, Cerdà V (2011) Applicability of multisyringe chromatography coupled to cold-vapor atomic fluorescence spectrometry for mercury speciation analysis. Anal Chem Acta 708(1–2):11–18
8. Panichev NA, Panicheva SE (2015) Determination of total mercury in fish and sea products by direct thermal decomposition atomic absorption spectrometry. Food Chem 166:432–441
9. Qiu ZL, Tang DY, Shu J, Chen GN, Tang DP (2016) Enzyme-triggered formation of enzyme-tyramine concatamers on nanogold-functionalized dendrimer for impedimetric detection of Hg (II) with sensitivity enhancement. Biosens Bioelectron 75: 108–115
10. Kumar VV, Anthony SP (2016) Highly selective colorimetric sensing of Hg^{2+} ions by label free AuNPs in aqueous medium across wide pH range. Sensor Actuat B-Chem 225:413–419
11. Wang LN, Liu FY, Sui N, Liu MH, Yu WW (2016) A colorimetric assay for Hg (II) based on the use of a magnetic aptamer and a hybridization chain reaction. Microchim Acta 183(11):2855–2860
12. Zhang H, Lei ZX, Fu X, Deng XC, Wang Q, Gu DY (2017) Hg^{2+}-triggered exonuclease III-assisted dual-cycle targets recycling amplification for label-free and ultrasensitive colorimetric detection of Hg^{2+}. Sensor Actuat B-Chem 246:896–903

13. He YQ, Zhang XB, Zeng K, Zhang SQ, Baloda M, Gurung AS, Liu GD (2011) Visual detection of Hg^{2+} in aqueous solution using gold nanoparticles and thymine-rich hairpin DNA probes. Biosens Bioelectron 26:4464–4470
14. Chen JH, Pan JF, Chen S (2017) A naked-eye colorimetric sensor for Hg^{2+} monitoring with cascade signal amplification based on target-induced conjunction of split DNAzyme fragments. Chem Commun 53:10224–10227
15. Lee JS, Mirkin CA (2008) Chip-based scanometric detection of mercuric ion using DNA-functionalized gold nanoparticles. Anal Chem 80:6805–6808
16. Chen JH, Zhou SG, Wen JL (2014) Disposable strip biosensor for visual detection of Hg^{2+} based on Hg^{2+}-triggered toehold binding and exonuclease III-assisted signal amplification. Anal Chem 86: 3108–3114
17. Liu S, Leng XQ, Wang X, Pei QQ, Cui XJ, Wang Y, Huang JD (2017) Enzyme-free colorimetric assay for mercury (II) using DNA conjugated to gold nanoparticles and strand displacement amplification. Microchim Acta 184(7):1969–1976
18. Hong MQ, Zeng BH, Li MY, Xu XQ, Chen GN (2018) An ultrasensitive conformation-dependent colorimetric probe for the detection of mercury(II) using exonuclease III-assisted target recycling and gold nanoparticles. Microchim Acta 185(72). https://doi.org/10.1007/s00604-017-2536-1
19. Li ZM, Zhong ZH, Liang RP, Qiu JD (2017) The colorimetric assay of DNA methyltransferase activity based on strand displacement amplification. Sensor Actuat B-Chem 238:626–632
20. Yang LZ, Yun W, Chen YL, Wu H, Liu XY, Fu M, Huang Y (2017) Ultrasensitive colorimetric and fluorometric detection of Hg (II) based on the use of gold nanoparticles and a catalytic hairpin assembly. Microchim Acta 184(12):4741–4747
21. Zarlaida F, Adlim M (2017) Gold and silver nanoparticles and indicator dyes as active agents in colorimetric spot and strip tests for mercury (II) ions: a review. Microchim Acta 184(1):45–58
22. Liu S, Wang Y, Xu W, Leng XQ, Wang HQ, Guo YN, Huang JD (2017) A novel sandwich-type electrochemical aptasensor based on GR-3D au and aptamer-AuNPs-HRP for sensitive detection of oxytetracycline. Biosens Bioelectron 88:181–187
23. Tian Y, Wang Y, Xu Y, Liu Y, Li D, Fan CH (2015) A highly sensitive chemiluminescence sensor for detecting mercury (II) ions: a combination of exonuclease III-aided signal amplification and graphene oxide-assisted background reduction. Sci China Chem 58(3):514–518
24. Wang SQ, Yang F, Jin D, Dai Q, Tu JY, Liu YJ, Ning Y, Zhang GJ (2017) Toehold mediated one-step conformation-switchable "signal-on" electrochemical DNA sensing enhanced with homogeneous enzymatic amplification. Anal Chem 89:5349–5356
25. Zhang YL, Tang LN, Yang F, Sun ZY, Zhang GJ (2015) Highly sensitive DNA-based fluorometric mercury (II) bioassay based on graphene oxide and exonuclease III-assisted signal amplification. Microchim Acta 182(7–8):1535–1541
26. Zuo XW, Zhang HG, Zhu Q, Wang WF, Feng J, Chen XG (2016) A dual-color fluorescent biosensing platform based on WS_2 nanosheet for detection of Hg^{2+} and Ag^{+}. Biosens Bioelectron 85:464–470
27. Yan FY, Kong DP, Luo YM, Ye QH, He JJ, Guo XF, Chen L (2016) Carbon dots serve as an effective probe for the quantitative determination and for intracellular imaging of mercury (II). Microchim Acta 183(5):1611–1618
28. Shi DC, Yan FY, Zhou XG, Zheng TC, Shi YY, Fu WG, Chen L (2016) Preconcentration and fluorometric detection of mercury ions using magnetic core-shell chitosan microspheres modified with a rhodamine spirolactam. Microchim Acta 183(1):319–327
29. Kamali KZ, Pandikumar A, Jayabal S, Ramaraj R, Lim HN, Ong BH, Bien CSD, Kee YY, Huang NM (2016) Amalgamation based optical and colorimetric sensing of mercury (II) ions with silver@graphene oxide nanocomposite materials. Microchim Acta 183(1):369–377
30. Noor AM, Rameshkumar P, Huang NM, Wei LS (2016) Visual and spectrophotometric determination of mercury (II) using silver nanoparticles modified with graphene oxide. Microchim Acta 183(2): 597–603
31. Shamsipur M, Safavi A, Mohammadpour Z, Ahmadi R (2016) Highly selective aggregation assay for visual detection of mercury ion based on competitive binding of sulfur-doped carbon nanodots to gold nanoparticles and mercury ions. Microchim Acta 183(7): 2327–2335